Atmos. Meas. Tech. Discuss., https://doi.org/10.5194/amt-2018-346
Manuscript under review for journal Atmos. Meas. Tech.
Discussion started: 13 November 2018

Atmospheric Measurement Techniques Discussions

Identification of Gas-phase Pyrolysis Products in a Prescribed Fire: Seminal Detections Using Infrared Spectroscopy for Naphthalene, Methyl Nitrite, Allene, Acrolein and Acetaldehyde**

Nicole K. Scharko[1], Ashley M. Oeck[1], Russell G. Tonkyn[1], Stephen P. Baker[2], Emily N. Lincoln[2], Joey Chong[3], Bonni M. Corcoran[3], Gloria M. Burke[3], David R. Weise[3], Tanya L. Myers[1], Catherine A. Banach[1], and Timothy J. Johnson[1*]

[1]Pacific Northwest National Laboratories, Richland, WA, USA
[2]USDA Forest Service, Rocky Mountain Research Station, Missoula, MT, USA
[3]USDA Forest Service, Pacific Southwest Research Station, Riverside, CA, USA

*To whom correspondence should be addressed: Timothy.Johnson@pnnl.gov

ABSTRACT

Volatile organic compounds (VOCs) are emitted from many sources, including wildland fire; VOCs have received heightened emphasis due to such gases' influential role in the atmosphere, as well as possible health effects. We have used extractive infrared (IR) spectroscopy on recent prescribed burns in longleaf pine stands and herein report seminal detection of five compounds using this technique. The newly reported IR detections include naphthalene, methyl nitrite, allene, acrolein and acetaldehyde. We discuss the approaches used for detection, particularly the software methods needed to fit the analyte and multiple (interfering) spectral components within the selected spectral micro-window(s). We also discuss the method's detection limits and individual species' context in terms of atmospheric chemistry.

Atmos. Meas. Tech. Discuss., https://doi.org/10.5194/amt-2018-346
Manuscript under review for journal Atmos. Meas. Tech.
Discussion started: 13 November 2018

Atmospheric Measurement Techniques Discussions

1. INTRODUCTION

Wildland fire releases significant quantities of trace gases into the environment (Crutzen et al., 1979; Andreae, 1991; Andreae et al., 2001; Akagi et al., 2011; Yokelson et al., 2013), and such gases can significantly influence atmospheric chemistry (Crutzen et al., 1990). In some parts of the world, wildfires are becoming more prevalent as well as increasing in impact (Miller et al., 2009; Turetsky et al., 2011). In many areas, however, prescribed burning is used as a preventive tool to reduce hazardous fuel buildups in an effort to reduce or eliminate the risk of such wildfires (Fernandes et al., 2003). Understanding the products associated with the burning of biomass has received considerable attention since the emissions can markedly impact the atmosphere. Fourier transform infrared (FTIR) spectroscopy is one technique that has been extensively used to identify and quantify gases emitted from burns, generally used in either an open path configuration (Burling et al., 2010; Akagi et al., 2014; Stockwell et al., 2014; Selimovic et al., 2018) or as an extractive method (Burling et al., 2011; Akagi et al., 2013; Akagi et al., 2014). Extractive systems typically use a long-path gas cell coupled to an FTIR instrument so as to increase the sensitivity. Such approaches have been quite successful; an increasing number of species continue to be identified and quantified due to the availability of reference gas-phase spectral libraries such as the PNNL library (Sharpe et al., 2004) or the HITRAN database (Gordon et al., 2017). Such libraries contain absorption cross-sections that make it possible to obtain quantitative results (i.e. mixing ratios) without the need for calibration gases. To the best of our knowledge, the actual list of biomass burning chemical species measured by FTIR has remained limited to ca. 36 compounds (Table 1); one goal of our research was to expand the list of chemical species to which infrared methods could be applied. All of the compounds detailed in this study have in fact been previously detected using other analytical methods (Karl et al., 2007; Yokelson et al., 2009; Akagi et al., 2013; Gilman

et al., 2015; Koss et al., 2018) such as proton-transfer-reaction time-of-flight mass spectrometry (PTR-ToF) (Koss et al., 2018) or gas chromatography-mass spectrometry (GC-MS) (Gilman et al., 2015), but have not as yet been identified using FTIR in burning investigations. We wished to determine if such species' signatures are also found sequestered in the IR spectra associated with wildland fire, and are thus amenable to IR detection. A second goal of the present study, whose biomass burning results are mostly detailed in a separate manuscript, is to better understand pyrolysis. Every wildland fire consists of two processes: thermal decomposition (pyrolysis) of solid wildland fuels into gases, tars, and char followed by combustion (oxidation) of the pyrolysis products resulting in flame gases and particulate matter in the smoke. Description and measurement (by any means) of the pyrolysis products adjacent to the flames of a wildland fire has seldom been performed. Non-intrusive measurement of the (pyrolysis) gases in the near-flame environment is desirable from both a scientific and safety perspective.

The major gas-phase compounds emitted from wildland fires are H_2O, CO_2, CO and CH_4 (Ward et al., 1991), all of which are easily identified and quantified via FTIR spectroscopy. Lightweight hydrocarbons, oxygenated hydrocarbons, nitrogen and sulfur species are all minor products that are also generated during burns (Talbot et al., 1988; Lobert et al., 1991; Yokelson et al., 1996). A host of more complex gases which can condense to form tar are also produced by pyrolysis of wildland fuels (Safdari et al., 2018; Amini et al., 2019). In a gas-phase IR spectrum of such species, however, the peaks associated with the minor products are often obfuscated by the more prominent features, such as those from CO_2, and can only be recognized in the residual of a multicomponent simulated fit once the larger features have been removed. Using data from a recent field campaign to measure pyrolysis products carried out in a pine forest at Fort Jackson, South Carolina, we have analyzed some of the IR spectra in more detail to search for the signatures

Atmos. Meas. Tech. Discuss., https://doi.org/10.5194/amt-2018-346
Manuscript under review for journal Atmos. Meas. Tech.
Discussion started: 13 November 2018

Atmospheric Measurement Techniques Discussions

of compounds not found in Table 1. As a partial guide of species for which to investigate, we searched for those species detected in previous thermogravimetric-FTIR (TG-FTIR) studies (Bassilakis et al., 2001; Taghizadeh et al., 2015). TG-FTIR experiments, however, are typically small-scale and carried out in controlled environments (in contrast to ambient conditions of prescribed burns or large-scale laboratory burns) and thus represent burns with different oxidative capacities / combustion efficiencies (Yokelson et al., 1996; Fang et al., 2006; Akagi et al., 2014). In this study, we have chosen to examine field fire spectra for species that can be detected and quantified via IR spectroscopy both to add to the list of compounds, but also to improve the characterization (and ultimately the detection limits) of the other species listed in Table 1. That is to say, fire IR spectra are very complex and contain many overlapping peaks; the success of the spectral analysis depends both on the selected spectral region and proper analysis of all compounds included in the fit to that domain. The chemometric results become more reliable as the signatures of all relevant species are included in the fit.

Table 1. Compounds previously detected in biomass burning studies using FTIR methods (Yokelson et al., 1996; Yokelson et al., 1997; Goode et al., 1999; Goode et al., 2000; Christian et al., 2003; Christian et al., 2004; Karl et al., 2007; Yokelson et al., 2009; Alves et al., 2010; Burling et al., 2010; Burling et al., 2011; Akagi et al., 2013; Akagi et al., 2014; Stockwell et al., 2014; Gilman et al., 2015; Hatch et al., 2017; Selimovic et al., 2018).

Compounds				
CO	NO	methanol	phenol	HCOOH
CO_2	NO_2	acetic acid	furaldehyde	peroxyacetyl nitrate**
CH_4	HONO	SO_2	hydroxyacetone	limonene
C_2H_2	NH_3	furan	1,3-butadiene	carbonyls as glyoxal
C_2H_4	HCN	H_2O	acetone	HCHO
C_2H_6	HCl	N_2O	isoprene	2-methylfuran*
C_3H_6	O_3**	OCS	glycolaldehyde	MVE (methyl vinyl ether)
C_4H_8				

* used in the fit, but not analyzed, ** secondary components found downwind

Atmos. Meas. Tech. Discuss., https://doi.org/10.5194/amt-2018-346
Manuscript under review for journal Atmos. Meas. Tech.
Discussion started: 13 November 2018

2. EXPERIMENTAL

2.1 Site description and sampling device

In early May 2018 seven prescribed fires were conducted in pine forests at U.S. Army Garrison Fort Jackson, adjacent to Columbia, South Carolina, at sites not far from previous smoke emission studies (Akagi et al., 2013; Weise et al., 2015). The forest overstory was primarily longleaf pine (*Pinus palustris* Mill.) and slash pine (*Pinus elliottii* Engelm.), while sparkleberry (*Vaccinium arboreum* Marshall) dominated the understory vegetation. During each burn, pyrolyzed gases emitted at the base of the flames before ignition were collected using an extractive probe and stored in 3-liter Summa canisters. This approach was performed to selectively collect pyrolysis gases prior to the onset of combustion. Details regarding the site description and sampling apparatus will be provided in a separate paper.

2.2 FTIR Spectrometer

Gases were analyzed in the laboratory (on the same day or the day following the fire) using an 8-meter multipass (White) cell (Bruker Optics, A136/2-L) mounted in the sample compartment of a Bruker Tensor 37 FTIR. Ten canisters were returned from the field to the laboratory and in turn connected to the gas cell via 3/8" stainless steel tubing. The tubing and gas cell were both heated to 70°C to prevent analyte adhesion to the inner surfaces. The White cell (White, 1942) was equipped with a pressure gauge and temperature probe, both of which were located on the gas outlet port; the thermocouple wire temperature probe extended into the White cell volume in order to more accurately measure the gas temperature. Prior to the start of the series of experiments, it was necessary to calibrate the path length of the variable path gas cell. Measurements of pure isopropyl alcohol (IPA, Sigma-Aldrich, 99.5%) at ten different pressures were collected and a Beer's Law plot was created to determine the length. The IR region from 3515 to 3290 cm^{-1} was

Atmos. Meas. Tech. Discuss., https://doi.org/10.5194/amt-2018-346
Manuscript under review for journal Atmos. Meas. Tech.
Discussion started: 13 November 2018

Atmospheric Measurement Techniques Discussions

integrated (Figure 1a), and the corresponding areas plotted as a function of the IPA pressure (converted to ppm at 760 Torr) multiplied by the PNNL reference library (Sharpe et al., 2004) integration area for a 1 ppm-meter IPA burden (Figure 1b). The slope is equal to the path length, which was determined to be 8.10 m.

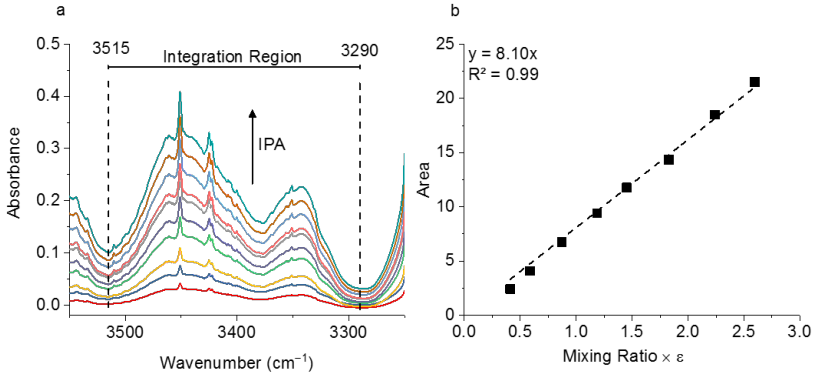

Figure 1. a) Multiple burden spectra of dry IPA for 10 measurements at varying pressures. The dashed lines represent the integration limits used for spectral integration. b) Calibration plot with regression line for IPA measurements. The slope of the line is the path length in meters.

The White cell contained the analyte smoke for the sample spectrum measurement, but was filled with ultra-high purity nitrogen gas for the reference spectrum measurement (Johnson et al., 2013). The FTIR interferometer, detector and sample compartments were purged with dry air from a dry-air generator. The Tensor 37 was equipped with a globar source, a KBr beamsplitter and a broadband liquid nitrogen cooled mercury cadmium telluride (MCT) detector, providing spectral coverage from 7,500 to 500 cm^{-1}. The spectral resolution was 0.6 cm^{-1} and a 2 mm Jacquinot aperture was used. The acquisition mode was set to double-sided, forward-backward. For the Fourier transform, the data were apodized with a Blackman-Harris 3-Term function using a zerofill factor of 4, and phase corrected via the Mertz (Mertz, 1967) method.

Atmos. Meas. Tech. Discuss., https://doi.org/10.5194/amt-2018-346
Manuscript under review for journal Atmos. Meas. Tech.
Discussion started: 13 November 2018

Atmospheric Measurement Techniques Discussions

134 **2.3 Quantitative Spectral Analysis**

135 The program used for quantitative spectral analysis was MALT5 (Griffith, 2016), which uses both
136 broadband reference spectra from PNNL (Sharpe et al., 2004; Johnson et al., 2006; Johnson et al.,
137 2009; Profeta et al., 2011; Lindenmaier et al., 2017) and absorption line intensities from HITRAN
138 (Gordon et al., 2017) (in units of $cm^{-1}/(\ molec \times cm^{-2}\ )$ to iteratively fit a simulated spectrum to
139 the measured spectrum by optimizing the fit so as to minimize the mean-squared residual, i.e. the
140 difference between the measured and simulated spectra. Parameters such as path length, resolution,
141 apodization, temperature, pressure, spectral domain, target compounds / overlapping compounds
142 are all used as inputs to the spectral fit. During the course of this study, MALT5 was used to
143 identify five gas-phase species emitted during the burns and quantify the gas mixing ratios via IR
144 spectroscopy for the first time. Part of the confirmation strategy is to process the experimental
145 spectra both with and without the target compound present in the fit and visually inspect the
146 corresponding residuals. Table 2 summarizes the IR-active vibrational mode used for each species
147 in the spectral fit (typically the species' strongest band in the longwave infrared window), along
148 with the spectral domain and a list of species with overlapping bands in that domain.

149

150

151

152

153

154

Atmos. Meas. Tech. Discuss., https://doi.org/10.5194/amt-2018-346
Manuscript under review for journal Atmos. Meas. Tech.
Discussion started: 13 November 2018

Atmospheric Measurement Techniques Discussions

Table 2. Gas-phase species identified via FTIR, vibrational assignments (Lord et al., 1952; Hollenstein et al., 1971; Ghosh et al., 1981; Hamada et al., 1985; Es-Sebbar et al., 2014; Chakraborty et al., 2016), and spectral domains used for spectral fit and quantitation.

Target compound	Vibrational bands used for analysis	Spectral region (cm^{-1})	Other species fit in the same region
Naphthalene	ν_{46} at 782.3 cm^{-1}	800–760	C_2H_2, CO_2, HCN and H_2O
Methyl nitrite	ν_8 at 841.1(*cis*) and 812.3 (*trans*) cm^{-1}	865–775	C_2H_2, CO_2, HCN, naphthalene, C_2H_4, allene, and H_2O
Allene	ν_{10} at 845.3 cm^{-1}	865–775	C_2H_2, CO_2, HCN, naphthalene, C_2H_4, methyl nitrite, and H_2O
Acrolein	ν_{10} at 1157.7 cm^{-1}	1200–1100	Acetic acid (CH_3COOH), furfural (C_4H_3OCHO), acetaldehyde , HCOOH, CH_4, C_2H_4, and H_2O
Acetaldehyde	ν_3 at 2716.2 cm^{-1}	2800–2650	CH_4, HCHO, C_2H_2, acrolein, and H_2O

2.4 Spectral Resolution

As mentioned in section 2.2, the spectral resolution was set to 0.6 cm^{-1}, which is the highest resolution obtainable with this instrument. There are many benefits, but also a few disadvantages to using higher resolution (Herget et al., 1979). Most importantly, the higher resolution allows one to resolve the narrow bands of key analytes and discriminate them from lines or bands of interferents. For example, in the present study the 782 cm^{-1} Q-branch of naphthalene was distinguished from the adjacent absorption lines of C_2H_2 [Naphthalene's IR bands and results are discussed in greater depth in Section 3.1]. If a lower resolution were used, then the deconvolution of naphthalene from C_2H_2 would have been compromised, perhaps unfeasible. To demonstrate, one of the experimental measurements collected at a resolution of 0.6 cm^{-1} was deresolved to 1, 2, and 4 cm^{-1} using a Gaussian profile as seen in Figure 2. Those spectra were processed by MALT5 to check for the presence of naphthalene. Figure 2 displays the measured spectra and the scaled reference spectra for C_2H_2 and naphthalene, and the corresponding residuals with and without naphthalene included in the fit for the a) original spectrum collected at 0.6 cm^{-1} and the

Atmos. Meas. Tech. Discuss., https://doi.org/10.5194/amt-2018-346
Manuscript under review for journal Atmos. Meas. Tech.
Discussion started: 13 November 2018

Atmospheric Measurement Techniques Discussions

deresolved spectra at b) 1 cm^{-1}, c) 2 cm^{-1}, and d) 4 cm^{-1}. With the reference spectra for the original 0.6 cm^{-1} measurement and the 1 cm^{-1} deresolved spectrum (Figure 2a and b), the absorption lines for C_2H_2 and naphthalene overlap, but the 782 cm^{-1} feature from naphthalene is still slightly visible in the original spectra. The naphthalene peak appears clearly in the residuals when it is not included in the fitting process, but is removed from the residual when naphthalene is included in the fit (discussed further below). As the resolution is reduced (Figures 2c and 2d), however, the features broaden and the distinction of the naphthalene peak from C_2H_2 and other minor components (i.e. CO_2, HCN, H_2O, spectra not shown) is compromised. The specificity between the compounds is lost and the confidence in the identification/quantification of the target species, particularly for the weaker absorbers, diminishes as the resolution decreases. The well-known benefits of using a lower resolution are that spectra can be acquired more quickly with an improved signal-to-noise ratio. For the present measurements, 0.6 cm^{-1} was deemed an appropriate resolution.

Atmos. Meas. Tech. Discuss., https://doi.org/10.5194/amt-2018-346
Manuscript under review for journal Atmos. Meas. Tech.
Discussion started: 13 November 2018

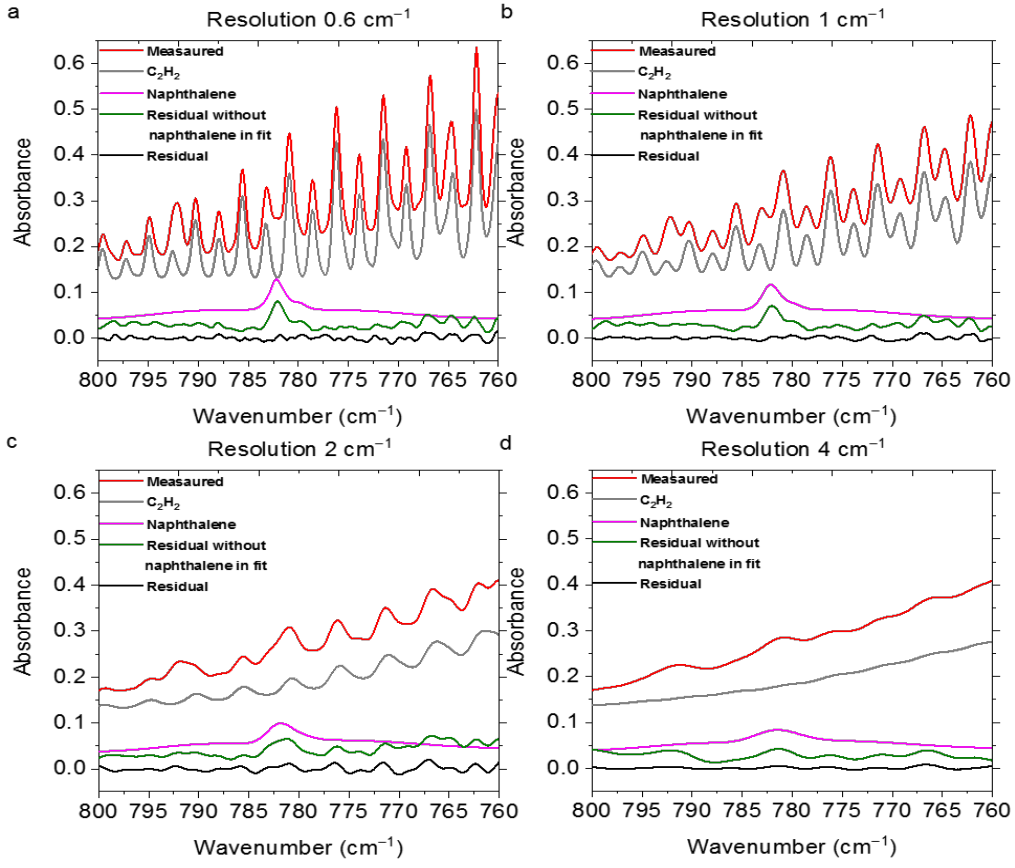

Figure 2. Measured and scaled reference spectra for C_2H_2 and naphthalene, and corresponding residuals with and without naphthalene included in the fit for the a) original spectrum collected at 0.6 cm^{-1} and the deresolved spectra at b) 1 cm^{-1}, c) 2 cm^{-1}, and d) 4 cm^{-1}. The reference spectra for CO_2, HCN and H_2O are not shown (HCN was not included in fit when the resolution was 4 cm^{-1}; for resolutions 1, 2 and 4 cm^{-1}, H_2O was not included in the fit when naphthalene was removed from the fit). Spectra are offset for clarity.

2.5 Detection Limits and Signal-to-noise Ratio

The detection limit values presented in this paper are not minimal signal-to-noise limits in the sense of a minimal spectral signal against a background of purely stochastic noise sources. In such cases, the noise sources are typically of comparable or higher frequencies than the signal (Johnson et al., 1991). Rather, the current limits represent the average detection limits for a spectral residual derived from a convoluted spectrum arising from a gas mixture of differing and fluctuating chemical composition. The residuals are due to the least-squares fit of (fluctuations in) the many

197 complex features arising from numerous chemicals. That is to say, the residual is not due to just
198 random instrumental noise, but instead, due to spectral features that can arise in the spectra, e.g.
199 imperfectly subtracted features from strong absorbers or unidentified absorbers. For that reason,
200 we report signal-to-residual, not signal-to-noise detection limits. The detection limits for each
201 compound in this study were thus derived using a value of three times the root-mean-square (RMS)
202 value of the residual calculated over the corresponding frequency range (e.g. 800–760 cm^{-1} was
203 used for naphthalene). The peak-to-peak noise is more sensitive to fluctuations in the fit with levels
204 typically 4 to 5× the RMS noise (Griffith et al., 2006). For the present data, however, the peak-to-
205 peak values ranged from 5 to 10× the RMS noise, thus suggesting the peak-peak values tend to
206 overstate the tractable noise level, i.e. understate the detection limit. The reported detection limits
207 are thus presumably higher than what would be estimated with an FTIR in clean air conditions (i.e.
208 only the analyte and dry air). Based on experience, the limits are typically far higher than what can
209 be obtained with IR laser sensors where the intrinsically narrow laser linewidths allow for the
210 probing of individual rotational-vibrational lines without drawing in overlapping spectral lines to
211 a congested spectral fit (Taubman et al., 2004; Wagner et al., 2011; Phillips et al., 2014). While
212 typically far more sensitive, such laser measurements can only analyze for one or a few species at
213 a time, as opposed to the 30+ species seen by the broadband FTIR measurements.

214 ## 3. RESULTS AND DISCUSSION

215 When modeling the burning process (Byram, 1959), complete combustion of 1 kg dry wood
216 produces 1.82 kg CO_2 and 0.32 kg H_2O for a total mass of products of 2.14 kg. Incomplete
217 combustion will yield additional products and less CO_2 and H_2O while combustion of wet fuels
218 (Byram, 1959) increases the amount of H_2O released. For infrared analysis of such smoke, much
219 of the challenge arises due not only to the large mole fractions of H_2O and CO_2, but the fact that

Atmos. Meas. Tech. Discuss., https://doi.org/10.5194/amt-2018-346
Manuscript under review for journal Atmos. Meas. Tech.
Discussion started: 13 November 2018

both H_2O vapor and CO_2 have strong features in the mid-IR that can clutter the spectrum rendering certain spectral regions unusable. For burning and other atmospheric studies, ideal compounds for detection via IR spectroscopy will thus have strong absorption coefficients that do not overlap with the fundamental bands of H_2O or CO_2, i.e. are in a spectral window or microwindow (Griffith, 1996; Esler et al., 2000; Smith et al., 2011) free of strong interferences. Here, we consider five such compounds emitted during this prescribed burn, but which had heretofore not been reported as being detected by FTIR. Individual compounds are discussed in turn regarding their formation mechanism(s), detectable IR features and spectral confirmation for this study, along with their potential fates and atmospheric impacts. Lastly, the results are briefly compared with literature values using emission ratios (mixing ratios of analyte to excess CO).

3.1 Naphthalene

Naphthalene ($C_{10}H_8$) is a polycyclic aromatic hydrocarbon (PAH) that is emitted from certain chemical industries as well as from the combustion of gasoline and oil (Jia et al., 2010). It is a condensable hydrocarbon also generated by biomass pyrolysis (Liu et al., 2017). There are a number of pyrolysis formation routes (Fairburn et al., 1990; Williams et al., 1999; Richter et al., 2000; Lu et al., 2004; Liu et al., 2017). One proposed mechanism is the generation of single ring aromatic compounds such as benzene, toluene and styrene via Diels-Alder reaction of alkenes; the single ring aromatic compound then combines with alkenes to form double-ring PAHs, such as naphthalene (Fairburn et al., 1990). Naphthalene may even undergo subsequent reactions to form still larger polyaromatics (Fairburn et al., 1990; Richter et al., 2000). Naphthalene has been detected (via GC-MS) in tars that were condensed from gas-phase pyrolysis products of both live and dead southeastern fuels, such as live oak (*Quercus virginiana*) and swamp bay (*Persea palustris*) (Safdari et al., 2018). It has been also detected (Hosseini et al., 2014; Aurell et al., 2017;

Atmos. Meas. Tech. Discuss., https://doi.org/10.5194/amt-2018-346
Manuscript under review for journal Atmos. Meas. Tech.
Discussion started: 13 November 2018

Atmospheric Measurement Techniques Discussions

Koss et al., 2018) in the gas-phase in laboratory burning experiments. The detection of gas-phase naphthalene from wildland fire emissions is thus not surprising, but this is the first report of its identification via IR spectroscopy. The best spectral feature for identification and quantification is the ν_{46} IR mode near 782.3 cm^{-1}, which corresponds to the H–C–C out-of-plane bend (Chakraborty et al., 2016). There are other bands at 3067.7 and 3058.0 cm^{-1} previously assigned to ν_{29} and ν_{17}, respectively (Chakraborty et al., 2016). Both of these modes have smaller absorption coefficients as compared to ν_{46}, however, and are located in the C–H stretching region, which is common to nearly all hydrocarbons and thus provides less specificity.

Figure 3 shows a prescribed burn spectrum in the region from 800 to 760 cm^{-1}. The primary spectral signatures in this plot are those of the R-branch rotational-vibrational lines associated with the ν_5 fundamental (Kabbadj et al., 1991) of C_2H_2, but there are also absorptions due to CO_2, HCN, H_2O (individual spectral contributions not shown) and naphthalene. When all of the spectral components except for naphthalene are included in the fitting process, the residual (green trace) displays a prominent feature at 782.3 cm^{-1}, which we ascribe to naphthalene. When naphthalene is included in the fit, the feature in question is removed as seen in the black trace of Figure 3.

Atmos. Meas. Tech. Discuss., https://doi.org/10.5194/amt-2018-346
Manuscript under review for journal Atmos. Meas. Tech.
Discussion started: 13 November 2018

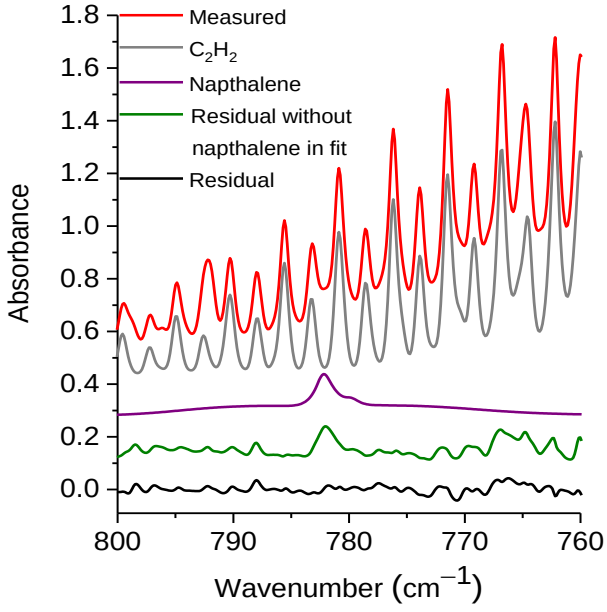

Figure 3. Measured spectrum, scaled reference spectra for C_2H_2 and naphthalene, and residuals with and without naphthalene included in the fit. For clarity, the spectral contributions for CO_2, HCN, and H_2O are not shown. All spectra are at 0.6 cm^{-1} resolution and have been offset. The calculated mixing ratio of naphthalene in this measured spectrum is 16.4 ± 0.6 ppm (values obtained from MALT5 software, and error represents standard error).

Table 3 presents the range of measured mixing ratios for naphthalene along with averaged detection limits for the 10 measurements collected during the prescribed burns as well as for the other four reported compounds. In the measurements, naphthalene's mixing ratios ranged from 1.4 to 19.9 ppm, and the averaged RMS-derived detection limit was 1.6 ± 0.5 ppm; different detection limits were observed for each spectrum. One of the measurements had a mixing ratio of 2.9 ppm, yet its RMS-derived detection limit was 3.7 ppm, and is thus below the estimated detection limit (bdl).

Atmos. Meas. Tech. Discuss., https://doi.org/10.5194/amt-2018-346
Manuscript under review for journal Atmos. Meas. Tech.
Discussion started: 13 November 2018

Atmospheric Measurement Techniques Discussions

Table 3. Calculated mixing ratios for ten canister FTIR measurements along with average estimated residual detection limits for the target compounds derived using 3 times the root-mean-square of the residual. Error bars represent the standard deviation (1σ) of the mean.

Target compound	Calculated mixing ratios (ppm)			Averaged detection limit (ppm) using root-mean-square (RMS) value of the residual
	Min	Max	Average	
Naphthalene*	1.4	19.9	8.5 ± 2.1	1.9 ± 0.5
Methyl nitrite*	2.3	21.0	8.7 ± 2.4	2.2 ± 0.4
Allene	2.2	37.8	13.1 ± 3.6	3.0 ± 0.6
Acrolein	14.7	125.7	43 ± 12	6.1 ± 1.5
Acetaldehyde	34.5	264.8	103 ± 27	11.7 ± 3.2

*One measurement was below the detection limit.

Naphthalene emitted from prescribed burns is thus clearly detectable using IR spectroscopy. The U.S. Environmental Protection Agency considers naphthalene a potential human carcinogen and a hazardous air pollutant (U.S. EPA). Once released, naphthalene may cycle in the atmosphere or accumulate in aquatic and terrestrial systems via wet/dry deposition or air-water gas exchange (Park et al., 2001). Gas-phase naphthalene's primary atmospheric loss mechanism is its reaction with the hydroxyl radical (OH) to form hydroxy-PAHs or nitro-PAHs in the presences of nitrogen oxides (Vione et al., 2004). The estimated atmospheric lifetime of naphthalene for reaction with OH is 6.8 hours (based on a 12-hour daytime OH level of 1.9×10^6 molecules cm^{-3}) (Arey, 1998).

3.2 Methyl Nitrite

A second compound detected for the first time in the wildland fire IR spectra was methyl nitrite ($CH_3ON=O$). Methyl nitrite has previously been observed in aged cigarette smoke (Schmeltz et al., 1977), and also the exhaust of engines fueled by methanol–diesel blends (Jonsson et al., 1982). It has also been observed as a minor product for the thermal decomposition of both nitrate esters (Boschan et al., 1955) and isopropyl nitrate at low temperatures and pressures (Griffiths et al., 1975). Methyl nitrite has also been detected in wildland fire emissions by GC-MS (Gilman et al.,

295 2015). Moreover, it has been observed that some nitrogen-containing organic compounds such as
296 acetonitrile (CH_3CN) and acrylonitrile (CH_2=CHCN) emitted from burns were directly correlated
297 to the fuel nitrogen content. However, methyl nitrite [and another oxygenated nitrogen organic
298 compound, isocyanic acid (HNCO)] did not show any significant dependency on fuel N-content
299 (Coggon et al., 2016). It has been suggested that methyl nitrite is only a minor direct product of
300 combustion (Finlayson-Pitts et al., 1992), but instead is generated *in situ* by the secondary reaction
301 of methanol (CH_3OH) with nitrogen dioxide (NO_2).

302 We also note that methyl nitrite is an oxidizing agent and is used as a rocket propellant. It is thus
303 plausible that the methyl nitrite detected in the present study was not a product of the fire, but
304 emanated from munitions used in training at Ft. Jackson. However, while the records of the
305 munitions used were not complete, a survey of these records did not indicate the use of methyl
306 nitrite in any munitions at the Ft. Jackson plots where the present burn samples were collected.

307 With regards to the IR spectra, methyl nitrite exists in equilibrium as a mixture of two conformers-
308 *cis* and *trans*; at room temperature (25°C) it is estimated as 58% *cis* and 42% *trans* (Bodenbinder
309 et al., 1994). We were able to use the same band associated with both conformers, namely the ν_8
310 band, which is at 841.1 cm^{-1} for the *cis* conformer and at 812.4 cm^{-1} for the *trans* conformer
311 (Ghosh et al., 1981). The ν_8 mode is associated with the N–O stretch and is very strong for both
312 conformers (Ghosh et al., 1981). We note that methyl nitrite also has very strong bands at 627.8
313 cm^{-1} (*cis*) for ν_9 ONO bending, as well as at 1620.1 cm^{-1} (*cis*) and 1677.4 cm^{-1} (*trans*) due to the
314 ν_3 N=O stretch (Ghosh et al., 1981). These bands, however, are of lesser utility for IR detection:
315 The ν_9 peak is masked by CO_2 bending mode lines, and the ν_3 peak is obfuscated by the H_2O
316 bending mode lines.

Atmos. Meas. Tech. Discuss., https://doi.org/10.5194/amt-2018-346
Manuscript under review for journal Atmos. Meas. Tech.
Discussion started: 13 November 2018

Atmospheric Measurement Techniques Discussions

317 The spectral region used for evaluation was 865–775 cm^{-1}, which contains the ν_8 band for both the
318 *cis* and *trans* conformers (Ghosh et al., 1981). Figure 4 shows the experimental spectrum from
319 the prescribed burn, along with the scaled reference spectra for the two major compounds used in
320 the fit: C_2H_2 and methyl nitrite. While important, other minor compounds, such as CO_2, HCN,
321 naphthalene, C_2H_4, allene, and H_2O, were also included in the analysis, but their spectral
322 contributions are not plotted. Additionally, Figure 4 displays the residuals both when methyl nitrite
323 was included in the fitting process and when it was excluded. Upon inspection of the residual
324 spectrum where it was excluded (green trace), it is clear that both the *cis* and *trans* features from
325 ν_8 are present and this confirms methyl nitrite in the pyrolysis smoke

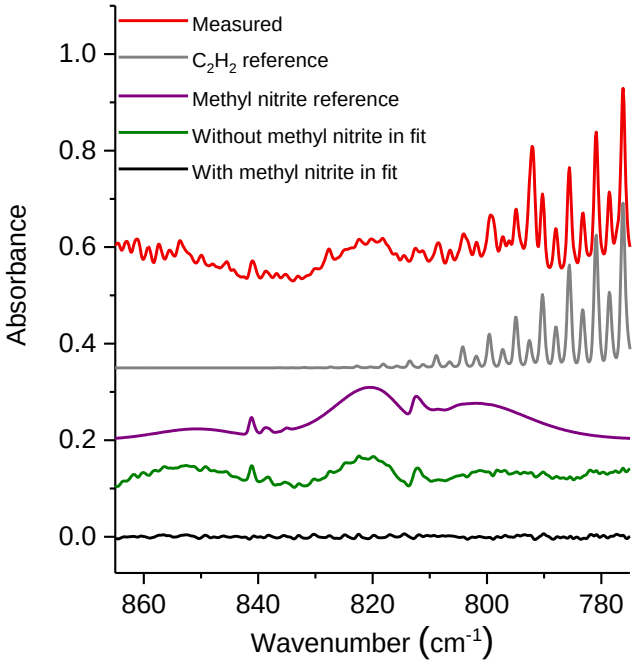

326
327
328 **Figure 4.** Measured experimental spectrum and the individual spectral contributions for the major
329 components (C_2H_2 and methyl nitrite) and residuals with and without methyl nitrite included in the fit. For
330 clarity, the spectral contributions for CO_2, HCN, naphthalene, C_2H_4, allene, and H_2O are not shown. All
331 spectra are at 0.6 cm^{-1} resolution and have been offset for clarity. The calculated mixing ratio of methyl
332 nitrite in this measured spectrum is 21.0 ± 0.1 ppm (values obtained from MALT5 software, and error
333 represents standard error).

Atmos. Meas. Tech. Discuss., https://doi.org/10.5194/amt-2018-346
Manuscript under review for journal Atmos. Meas. Tech.
Discussion started: 13 November 2018

The mixing ratio and RMS-derived detection limit for methyl nitrite for the displayed experimental spectrum in Figure 4 are 21.0 ppm and 1.4 ppm, respectively. The range for the mixing ratios and the averaged detection limits for methyl nitrite are summarized in Table 3. Methyl nitrite was detected with confidence in 9 of the 10 measurements; only one of the measurements was below the RMS-derived detection limit.

We report the detection via IR spectroscopy of methyl nitrite in wildland fire emissions not only because it is novel, but also because of its influential role in atmospheric chemistry: Methyl nitrite is a photochemical source of OH. In the atmosphere it undergoes photolysis to form the methoxy radical (CH_3O) and nitric oxide (NO) with a quantum yield near unity (Cox et al., 1980). At solar noon, the photolytic lifetime is only 10–15 min (Seinfeld et al., 2012). The photogenerated methoxy radical then undergoes subsequent reactions leading to the formation of OH. In turn, both OH and NO contribute to the production of ozone (Finlayson-Pitts et al., 1999).

3.3 Allene

Allene (1,2-propadiene, $CH_2=C=CH_2$) is of high symmetry (D_{2d}) and has the two methylene groups with their H–C–H planes at right angles to each other (Lord et al., 1952). The compound has previously been detected in biomass burning grab samples using GC (Akagi et al., 2013). Allene is a proposed precursor in the burning process that contributes to the formation of both aromatic compounds and soot (Frenklach et al., 1983; Frenklach et al., 1988). Lifshitz et al. have observed (at temperatures ranging from 757–847°C) that the structural isomerization of allene and propyne ($CH_2=C=CH_2 \leftrightarrow CH_3–C\equiv CH$) will take place via a unimolecular reaction faster than the decomposition reaction (Lifshitz et al., 1975). Additionally, these same authors investigated the pyrolysis of allene and propyne and observed that C_2H_4 was generated from allene while CH_4 and C_2H_2 were mainly formed from propyne (Lifshitz et al., 1976). Unfortunately, the strongest IR

Atmos. Meas. Tech. Discuss., https://doi.org/10.5194/amt-2018-346
Manuscript under review for journal Atmos. Meas. Tech.
Discussion started: 13 November 2018

Atmospheric Measurement Techniques Discussions

band for propyne (near 634 cm^{-1}) is obscured by CO_2 bending mode lines. Due to the interferences we cannot with confidence identify propyne in the measurements; we can, however, detect allene. In the mid-IR, allene has several strong rotational-vibrational lines near 845 cm^{-1} associated with the sub-bands of the perpendicular band ν_{10}, which is due to CH_2 rocking (Lord et al., 1952). Additionally, allene has a moderately strong band at 1958.6 cm^{-1} due to the ν_6 C–C stretching (Lord et al., 1952). However, the ν_6 band is not useful for detection due to interference from the H_2O bending mode lines.

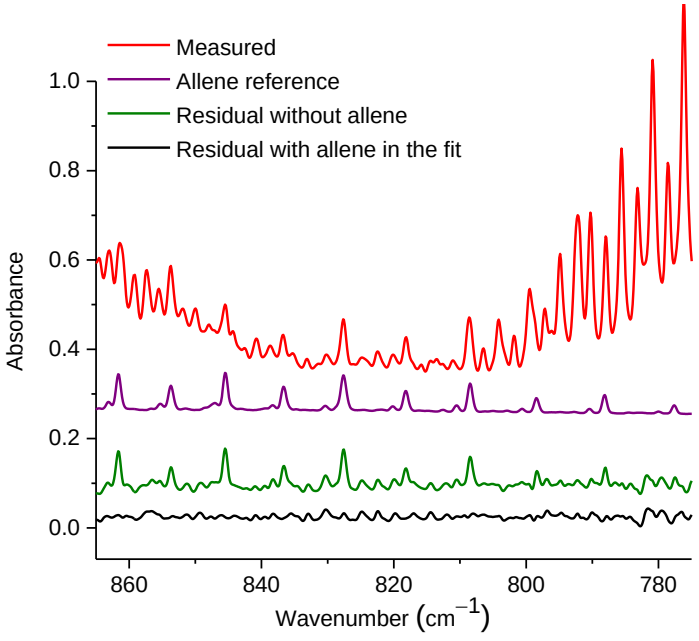

Figure 5. Measured absorbance spectrum and residual with and without allene included in the fit, along with the scaled reference spectrum for allene. For clarity, the spectral contributions for C_2H_2, CO_2, HCN, naphthalene, C_2H_4, methyl nitrite, and H_2O are not shown. All spectra are at 0.6 cm^{-1} resolution and have been offset for clarity. The calculated mixing ratio of allene in this measured spectrum is 37.8 ± 0.6 ppm (values obtained from MALT5 software, and error represents standard error).

Figure 5 shows the measured absorbance spectrum, scaled allene reference spectrum and the associated residual with and without allene included in the fit. The absorption lines associated with allene are clearly seen in the resulting spectrum when allene is not included in the fit (green

374 trace), thus confirming that allene is one of the primary components contributing to the features in
375 this spectral domain. For the experimental spectrum displayed in Figure 5, the calculated mixing
376 ratio for allene is 37.8 ppm and the RMS-derived detection limit is 5.4 ppm.
377
378 Unlike naphthalene and methyl nitrite, allene is not considered a hazardous air pollutant nor is it a
379 photochemical source of OH. Major loss processes for alkenes include reactions with OH, NO_3
380 radical and O_3 (Atkinson et al., 2003). Specifically for allene, the lifetime (calculated from rate
381 constants from Atkinson et al., 2003, and based on a 12-hour daytime OH level of 1.9×10^6
382 molecules cm^{-3} and 24-hour O_3 average of 7×10^{11} molecules cm^{-3}) with respect to OH and O_3
383 reactions are 1.2 and 89.4 days, respectively. The reaction between OH and allene involves the
384 initial addition of OH to one of the C=C bonds generating a hydroxyalkyl radical, which then may
385 undergo subsequent reactions (i.e. reaction with O_2 forming hydroxyalkyl peroxy radical)
386 contributing to the propagation of radicals in the atmosphere (Atkinson et al., 2003; Daranlot et
387 al., 2012).
388
389 **3.4 Acrolein and Acetaldehyde**

390 The two aldehydes, acrolein (CH_2=CHCHO) and acetaldehyde (CH_3CHO), have also been
391 identified in the burning IR spectra. It has been proposed that both acrolein and acetaldehyde are
392 formed from the pyrolysis of cellulose (a major constituent of biomass) via the intermediate
393 glycerol, which is a moiety in the structure of levoglucosan, a known pyrolysis product of cellulose
394 (Stein et al., 1983). Stein et al. observed that acrolein, acetaldehyde and CO were the initial
395 decomposition products for the pyrolysis of glycerol (Stein et al., 1983). Both of these compounds

have been detected in previous wildland fires studies via methods such as GC (Akagi et al., 2013) or PTR-ToF (Brilli et al., 2014; Koss et al., 2018), but have not yet been identified via IR.

Acrolein, the simplest unsaturated carbonyl, exists in two forms, *s-cis* and *s-trans*, with *s-trans* being the more stable, and consequently the more abundant conformer (Wagner et al., 1957). It has been estimated that the fractions of *s-cis* and *s-trans* are about 4 and 96% at 20°C, and 7 and 93% at 100°C, respectively (Alves et al., 1971). The largest IR feature for acrolein is the ν_5 C=O stretch (Hamada et al., 1985) at 1724.1 cm^{-1}, but this band is heavily overlapped by water lines. There is also the ν_{16} band (Hamada et al., 1985) at 958.8 cm^{-1}, but this feature overlaps with multiple other strongly absorbing compounds, such as C_2H_4. We have therefore focused acrolein's analysis using the ν_{10} band (C–C stretch) (Hamada et al., 1985) at 1157.7 cm^{-1}.

Figure 6 displays the very congested biomass burning spectrum with individual contributions for several species included in the fit [contributions for furfural (C_4H_3OCHO), acetaldehyde, CH_4, and C_2H_4 are included, but not plotted] as well as the residual with and without acrolein included in the fitting process. When acrolein is not included in the fit, features (both near 1168 and at 1157.7 cm^{-1}) that resemble acrolein are observed in the residual spectrum as seen in the green trace in Figure 6. When acrolein is included in the fit, the features in question are removed. For acrolein, no mixing ratios were observed below the RMS-derived detection limits.

Atmos. Meas. Tech. Discuss., https://doi.org/10.5194/amt-2018-346
Manuscript under review for journal Atmos. Meas. Tech.
Discussion started: 13 November 2018

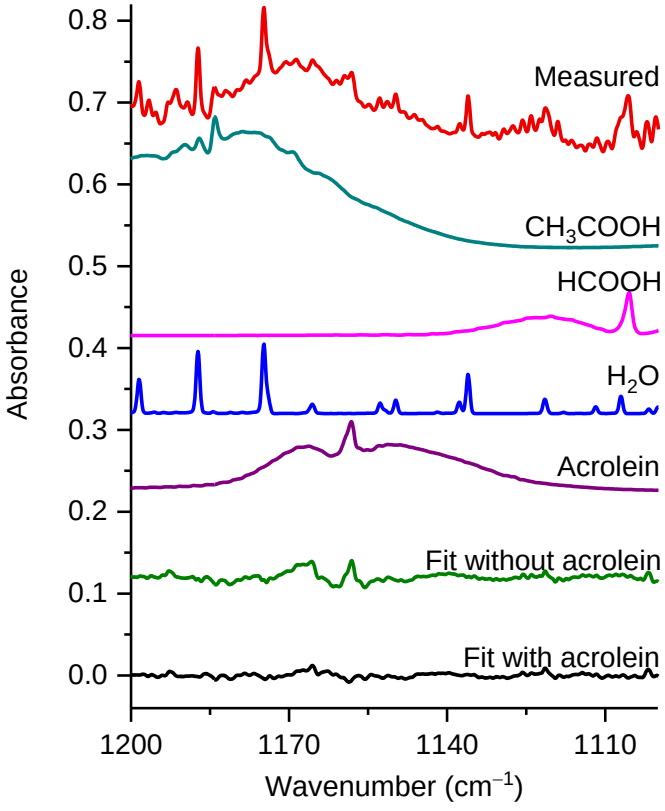

Figure 6. Measured spectrum and the individual spectral contributions for the major components and associated residual with and without acrolein included in the fit. For clarity, the spectral contributions for furfural (C_4H_3OCHO), acetaldehyde, CH_4, and C_2H_4 are not shown. All spectra are at 0.6 cm^{-1} resolution and have been offset for clarity. The calculated mixing ratio of acrolein in this measured spectrum is 99.9 ± 3.0 ppm (values obtained from MALT5 software, and error represents standard error).

Similar to acrolein, acetaldehyde has its strongest IR feature due to the C=O stretch (Hollenstein et al., 1971), with ν_4 found at 1746.1 cm^{-1}. Again, due to the presence of water lines in the spectrum, this features is not practical for detection. The aldehyde ν_3 C–H stretching band (Hollenstein et al., 1971) at 2716.2 cm^{-1} was instead used for analysis. Figure 7 shows the measured and fitted spectra as well as the spectral contributions of the major individual components used to calculate the fitted spectrum and the corresponding residual. Other minor

Atmos. Meas. Tech. Discuss., https://doi.org/10.5194/amt-2018-346
Manuscript under review for journal Atmos. Meas. Tech.
Discussion started: 13 November 2018

Atmospheric Measurement Techniques Discussions

427 components, such as acrolein, C_2H_2 and H_2O, were also included in the fit, but their reference
428 spectra are not displayed in Figure 7. The spectral profile of acetaldehyde with its P and R branches
429 of ν_3 is easily discernable even before deconvolution of the measured spectrum. Similar to
430 acrolein, all of the mixing ratios for acetaldehyde were above the RMS-derived detection limit.

431

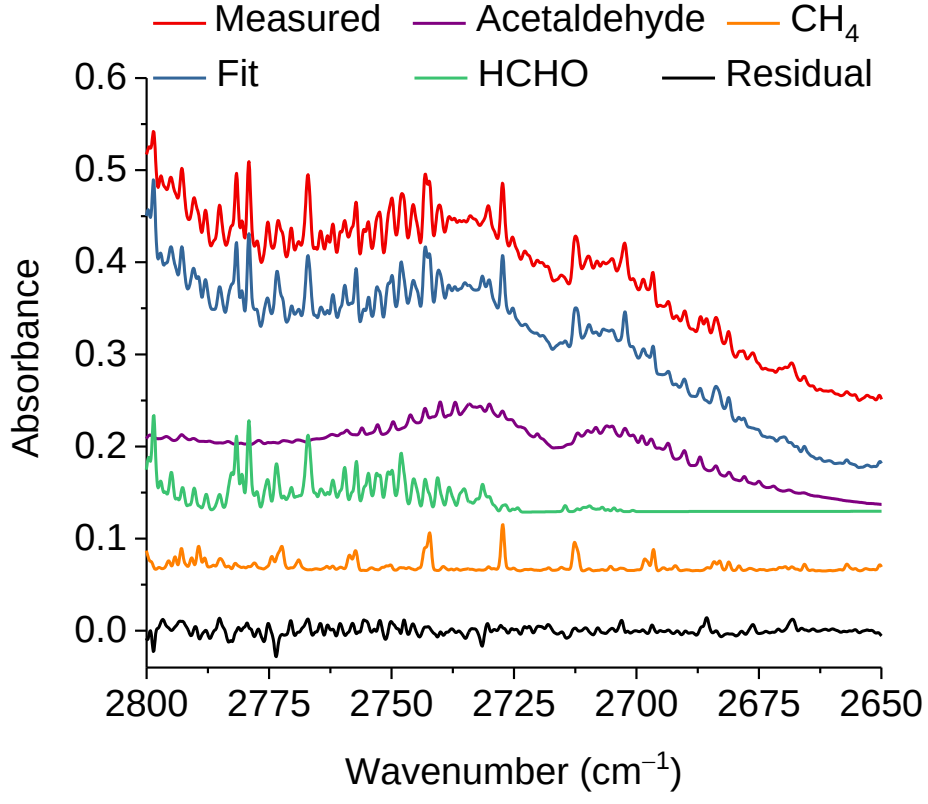

432
433 **Figure 7.** Measured and fitted spectra as well as the individual components (for clarity, the spectral
434 contributions for acrolein, C_2H_2, H_2O are not shown) and associated residual in the spectral region 2800-
435 2650 cm^{-1}. All spectra are at 0.6 cm^{-1} resolution and have been offset for clarity. The calculated mixing
436 ratio of acetaldehyde in this measured spectrum is 252.8 ± 5.5 ppm (values obtained from MALT5 software,
437 and error represents standard error).
438
439 Similar to naphthalene, the U.S. EPA considers both acrolein and acetaldehyde to be hazardous
440 air pollutants (U.S. EPA). Acrolein is toxic to humans, and when inhaled may cause upper
441 respiratory irritation. Acetaldehyde will irritate the eyes, skin and the respiratory tract and is

considered a potential human carcinogen (U.S. EPA). Once released into atmosphere, such aldehydes can either react with O_3 or OH, or undergo photolysis (Seinfeld et al., 2012). For acrolein, OH reaction is the major loss process with a lifetime of 2.4 hours based on a 12-hour daytime OH level of 1.9×10^6 molecules cm^{-3}, (Gierczak et al., 1997) forming products such as CO, CO_2, HCHO, glycolaldehyde (Johnson et al., 2013) and acryloylperoxynitrate (APAN) (Orlando et al., 2002). Similarly, acetaldehyde's lifetime is dominated by OH loss, and that reaction generates HCHO and CO as well as peroxyacetylnitrate (PAN) (D'Anna et al., 2003). Acetaldehyde's estimated tropospheric lifetimes with respect to OH reaction and photolysis are 10 hours (Atkinson et al., 2003) and 5 days (Seinfeld et al., 2012), respectively.

3.5 Comparison to Other Measurements

Preliminary emission ratios (relative to CO) for the reported compounds are compared to those reported in previous wildland burning investigations: Table 4 displays the average emission ratios and the standard deviations (1σ) for this study as well as emission ratios reported by Koss et al. (2018), Ferek et al. (1998), Brilli et al. (2014), and Gilman et al. (2015). As shown in the table, there is significant variation between the studies due to multiple factors such as different fuel types, analytical methods, sampling approaches and experimental conditions. For example, the study by Ferek et al. (1998) focused on the collection of airborne samples, while Brilli et al. (2014) measured gases under nocturnal conditions using a ground-based system. Inspection of the table shows that the measured emission ratio values are not unprecedented, but are within range of previous measurements. Because they have the same molar mass, the mass spectrometric techniques in some cases cannot distinguish allene from propyne.

Atmos. Meas. Tech. Discuss., https://doi.org/10.5194/amt-2018-346
Manuscript under review for journal Atmos. Meas. Tech.
Discussion started: 13 November 2018

Atmospheric Measurement Techniques Discussions

464 **Table 4.** Emission ratios relative to CO and standard deviations (1σ) for the present study and for
465 three other previously published biomass burning studies.

Target compounds	Present average emission ratios to CO (ppb/ppm)	Koss et al. (2018) fire-integrated emission ratio to CO (ppb/ppm)	Ferek et al. (1998) emission ratio to CO (ppb/ppm)	Brilli et al. (2014) emission ratios to CO (ppb/ppm)	Gilman et al. (2015) discrete emission ratios to CO (ppb/ppm)		
					South-western fuels	South-eastern fuels	Northern fuels
Method	FTIR	PTR-ToF-MS	GC-FID*	PTR-ToF-MS	GC-MS	GC-MS	GC-MS
Naphthalene	0.79 (0.47)	0.20 (0.16)	n/a	n/a	0.0070 (0.0048)	0.0040 (0.0050)	0.022 (0.012)
Methyl nitrite	0.94 (0.85)	n/a	n/a	n/a	0.9 (1.1)	0.52 (0.51)	0.76 (0.90)
Acrolein	4.0 (1.8)	5.4 (3.0)	n/a	3.14 (0.12)	0.82 (0.68)	1.31 (0.88)	3.5 (1.7)
Acetaldehyde	9.4 (3.6)	7.4 (5.2)	n/a	37.3 (1.4)	1.6 (1.2)	2.8 (1.8)	5.5 (3.6)
Allene (Propadiene)**	1.05 (0.24)	n/a	0.1 (0.1)	8.73 (0.28)	n/a	n/a	n/a

466 *GC-FID is gas chromatography with flame ionization detector
467 **Brilli et al. (2014) use both 1-propyne and propadiene to represent C_3H_4. Gilman et al. (2015) report emission
468 ratios for propyne, but not allene.
469

470 ## 4. SUMMARY

471 Gas-phase compounds with appreciable band intensities and appreciable concentrations can be
472 both identified and quantified using IR spectroscopy. We have used such spectral information for
473 seminal IR detection of five compounds generated during prescribed forest fire burns. Deriving
474 the mixing ratios from the congested spectra obtained from wildland smoke samples is more
475 challenging due to the multiple overlapping spectral features: Sophisticated software and analysis
476 are required in carefully selected spectral windows. We have reported seminal IR detection of five
477 molecules that had previously not been observed by FTIR in ambient measurements of wildland
478 emissions. Most of the compounds (excluding acetaldehyde), had their primary features become
479 apparent only after the larger spectral features had been fitted and subtracted.

480

481

ACKNOWLEDGMENT

We gratefully acknowledge support from the Department of Defense's Strategic Environmental Research and Development Program (SERDP), Project RC-2640 and gratefully thank our sponsor for their support. PNNL is operated for the U.S. Department of Energy by the Battelle Memorial Institute under contract DE-AC06-76RLO 1830. We thank Professor Valerie Young of Ohio University for loan of the canisters. 1830. We thank Prof. David W. T. Griffith for his valuable guidance and direction using the MALT5 program for spectral analysis. We kindly thank John Maitland and colleagues at Fort Jackson for conducting the burns and hosting the scientific mission, and Olivia Williams for assistance with the MALT calculations. Lastly, we are most grateful to Professor Michael L. Myrick and his colleagues at the University of South Carolina for allowing us to use their laboratories and for their helpful assistance during the campaign.

5. REFERENCES

Akagi, S. K., Burling, I. R., Mendoza, A., Johnson, T. J., Cameron, M., Griffith, D. W. T., Paton-Walsh, C., Weise, D. R., Reardon, J., and Yokelson, R. J.: Field measurements of trace gases emitted by prescribed fires in southeastern US pine forests using an open-path FTIR system, Atmos. Chem. Phys., 14, 199-215, 2014.

Akagi, S. K., Yokelson, R. J., Burling, I. R., Meinardi, S., Simpson, I., Blake, D. R., McMeeking, G. R., Sullivan, A., Lee, T., Kreidenweis, S., Urbanski, S., Reardon, J., Griffith, D. W. T., Johnson, T. J., and Weise, D. R.: Measurements of reactive trace gases and variable O_3 formation rates in some South Carolina biomass burning plumes, Atmos. Chem. Phys., 13, 1141-1165, 2013.

Akagi, S. K., Yokelson, R. J., Wiedinmyer, C., Alvarado, M. J., Reid, J. S., Karl, T., Crounse, J. D., and Wennberg, P. O.: Emission factors for open and domestic biomass burning for use in atmospheric models, Atmos. Chem. Phys., 11, 4039-4072, 2011.

Alves, A. C. P., Christoffersen, J., and Hollas, J. M.: Near ultra-violet spectra of the *s-trans* and a second rotamer of acrolein vapour, Mol. Phys., 20, 625-644, 1971.

Alves, C. A., Gonçalves, C., Pio, C. A., Mirante, F., Caseiro, A., Tarelho, L., Freitas, M. C., and Viegas, D. X.: Smoke emissions from biomass burning in a Mediterranean shrubland, Atmos. Environ., 44, 3024-3033, 2010.

Amini, E., Safdari, M.-S., DeYoung, J. T., Weise, D. R., and Fletcher, T. H.: Characterization of pyrolysis products from slow pyrolysis of live and dead vegetation native to the southern United States, Fuel, 235, 1475-1491, 2019.

514 Andreae, M. O.: Biomass burning: its history, use, and distribution and its impact, Global Biomass
515 Burning: Atmospheric, Climatic, and Biospheric Implications [JS Levine (Ed.)]. Cambridge, MA, MIT
516 Press, 1991.
517 Andreae, M. O., and Merlet, P.: Emission of trace gases and aerosols from biomass burning, Global
518 Biogeochem. Cycles, 15, 955-966, 2001.
519 Arey, J.: Atmospheric reactions of PAHs including formation of nitroarenes. PAHs and related
520 compounds, Springer: 347-385, 1998.
521 Atkinson, R., and Arey, J.: Atmospheric degradation of volatile organic compounds, Chem. Rev., 103,
522 4605-4638, 2003.
523 Aurell, J., Gullett, B. K., Tabor, D., and Yonker, N.: Emissions from prescribed burning of timber slash
524 piles in Oregon, Atmos. Environ., 150, 395-406, 2017.
525 Bassilakis, R., Carangelo, R. M., and Wojtowicz, M. A.: TG-FTIR analysis of biomass pyrolysis, Fuel,
526 80, 1765-1786, 2001.
527 Bodenbinder, M., Ulic, S. E., and Willner, H.: A Gas-Phase and Matrix Isolation Study of the Equilibrium
528 CH_3ONO (cis) ⇄ CH_3ONO (trans) by FTIR Spectroscopy, J. Phys. Chem., 98, 6441-6444, 1994.
529 Boschan, R., Merrow, R. T., and van Dolah, R. W.: The chemistry of nitrate esters, Chem. Rev., 55, 485-
530 510, 1955.
531 Brilli, F., Gioli, B., Ciccioli, P., Zona, D., Loreto, F., Janssens, I. A., and Ceulemans, R.: Proton Transfer
532 Reaction Time-of-Flight Mass Spectrometric (PTR-TOF-MS) determination of volatile organic
533 compounds (VOCs) emitted from a biomass fire developed under stable nocturnal conditions, Atmos.
534 Environ., 97, 54-67, 2014.
535 Burling, I. R., Yokelson, R. J., Akagi, S. K., Urbanski, S. P., Wold, C. E., Griffith, D. W. T., Johnson, T.
536 J., Reardon, J., and Weise, D. R.: Airborne and ground-based measurements of the trace gases and
537 particles emitted by prescribed fires in the United States, Atmos. Chem. Phys., 11, 12197-12216, 2011.
538 Burling, I. R., Yokelson, R. J., Griffith, D. W. T., Johnson, T. J., Veres, P., Roberts, J. M., Warneke, C.,
539 Urbanski, S. P., Reardon, J., Weise, D. R., Hao, W. M., and de Gouw, J.: Laboratory measurements of
540 trace gas emissions from biomass burning of fuel types from the southeastern and southwestern United
541 States, Atmos. Chem. Phys., 10, 11115-11130, 2010.
542 Byram, G. M.: Combustion of forest fuels. In 'Forest fire: control and use'.(Ed. KP Davis) pp. 61–89,
543 McGraw-Hill: New York, 1959.
544 Chakraborty, S., Banik, S., and Das, P. K.: Anharmonicity in the vibrational spectra of naphthalene and
545 naphthalene-d_8: Experiment and theory, J. Phys. Chem. A, 120, 9707-9718, 2016.
546 Christian, T. J., Kleiss, B., Yokelson, R. J., Holzinger, R., Crutzen, P. J., Hao, W. M., Saharjo, B. H., and
547 Ward, D. E.: Comprehensive laboratory measurements of biomass-burning emissions: 1. Emissions
548 from Indonesian, African, and other fuels, J. Geophys. Res. Atmos., 108, 2003.
549 Christian, T. J., Kleiss, B., Yokelson, R. J., Holzinger, R., Crutzen, P. J., Hao, W. M., Shirai, T., and
550 Blake, D. R.: Comprehensive laboratory measurements of biomass-burning emissions: 2. First
551 intercomparison of open-path FTIR, PTR-MS, and GC-MS/FID/ECD, J. Geophys. Res. Atmos., 109,
552 2004.
553 Coggon, M. M., Veres, P. R., Yuan, B., Koss, A., Warneke, C., Gilman, J. B., Lerner, B. M., Peischl, J.,
554 Aikin, K. C., Stockwell, C. E., Hatch, L. E., Ryerson, T. B., Roberts, J. M., Yokelson, R. J., and de
555 Gouw, J. A.: Emissions of nitrogen-containing organic compounds from the burning of herbaceous
556 and arboraceous biomass: Fuel composition dependence and the variability of commonly used nitrile
557 tracers, Geophys. Res. Lett., 43, 9903-9912, 2016.
558 Cox, R. A., Derwent, R. G., Kearsey, S. V., Batt, L., and Patrick, K. G.: Photolysis of methyl nitrite:
559 Kinetics of the reaction of the methoxy radical with O_2, J. Photochem., 13, 149-163, 1980.
560 Crutzen, P. J., and Andreae, M. O.: Biomass burning in the tropics: Impact on atmospheric chemistry and
561 biogeochemical cycles, Science, 250, 1669-1678, 1990.
562 Crutzen, P. J., Heidt, L. E., Krasnec, J. P., Pollock, W. H., and Seiler, W.: Biomass burning as a source of
563 atmospheric gases CO, H_2, N_2O, NO, CH_3Cl and COS, Nature, 282, 253, 1979.

564 D'Anna, B., Bakken, V., Beukes, J. A., Nielsen, C. J., Brudnik, K., and Jodkowski, J. T.: Experimental
565 and theoretical studies of gas phase NO_3 and OH radical reactions with formaldehyde, acetaldehyde
566 and their isotopomers, Phys. Chem. Chem. Phys., 5, 1790-1805, 2003.
567 Daranlot, J., Hickson, K. M., Loison, J.-C., Méreau, R., Caralp, F., Forst, W., and Bergeat, A.: Gas-Phase
568 Kinetics of the Hydroxyl Radical Reaction with Allene: Absolute Rate Measurements at Low
569 Temperature, Product Determinations, and Calculations, J. Phys. Chem. A, 116, 10871-10881, 2012.
570 Es-Sebbar, E., Jolly, A., Benilan, Y., and Farooq, A.: Quantitative mid-infrared spectra of allene and
571 propyne from room to high temperatures, J. Mol. Spectrosc., 305, 10-16, 2014.
572 Esler, M. B., Griffith, D. W. T., Wilson, S. R., and Steele, L. P.: Precision trace gas analysis by FT-IR
573 spectroscopy. 1. Simultaneous analysis of CO_2, CH_4, N_2O, and CO in air, Anal. Chem., 72, 206-215,
574 2000.
575 Fairburn, J. A., Behie, L. A., and Svrcek, W. Y.: Ultrapyrolysis of n-hexadecane in a novel micro-reactor,
576 Fuel, 69, 1537-1545, 1990.
577 Fang, M. X., Shen, D. K., Li, Y. X., Yu, C. J., Luo, Z. Y., and Cen, K. F.: Kinetic study on pyrolysis and
578 combustion of wood under different oxygen concentrations by using TG-FTIR analysis, J. Anal. Appl.
579 Pyrolysis, 77, 22-27, 2006.
580 Fernandes, P. M., and Botelho, H. S.: A review of prescribed burning effectiveness in fire hazard
581 reduction, Int. J. Wildland Fire, 12, 117-128, 2003.
582 Finlayson-Pitts, B. J., and Pitts Jr, J. N.: Chemistry of the upper and lower atmosphere: theory,
583 experiments, and applications, Elsevier, 1999.
584 Finlayson-Pitts, B. J., Pitts Jr, J. N., and Lloyd, A. C.: Comment on" A study of the stability of methanol-
585 fueled vehicle emissions in Tedlar bags", Environ. Sci. Technol., 26, 1668-1670, 1992.
586 Frenklach, M., Taki, S., Durgaprasad, M. B., and Matula, R. A.: Soot formation in shock-tube pyrolysis
587 of acetylene, allene, and 1, 3-butadiene, Combust. Flame, 54, 81-101, 1983.
588 Frenklach, M., Yuan, T., and Ramachandra, M. K.: Soot formation in binary hydrocarbon mixtures,
589 Energy Fuels, 2, 462-480, 1988.
590 Ghosh, P. N., and Günthard, H. H.: Cis and trans methyl nitrite: Gas phase ir spectra, band envelope
591 analysis, hot band progressions and assignments, Spectrochim. Acta A Mol. Spectrosc., 37, 347-363,
592 1981.
593 Gierczak, T., Burkholder, J. B., Talukdar, R. K., Mellouki, A., Barone, S. B., and Ravishankara, A. R.:
594 Atmospheric fate of methyl vinyl ketone and methacrolein, J. Photochem. Photobiol., A 110, 1-10,
595 1997.
596 Gilman, J. B., Lerner, B. M., Kuster, W. C., Goldan, P. D., Warneke, C., Veres, P. R., Roberts, J. M., de
597 Gouw, J. A., Burling, I. R., and Yokelson, R. J.: Biomass burning emissions and potential air quality
598 impacts of volatile organic compounds and other trace gases from fuels common in the US, Atmos.
599 Chem. Phys., 15, 13915-13938, 2015.
600 Goode, J. G., Yokelson, R. J., Susott, R. A., and Ward, D. E.: Trace gas emissions from laboratory
601 biomass fires measured by open-path Fourier transform infrared spectroscopy: Fires in grass and
602 surface fuels, J. Geophys. Res. Atmos., 104, 21237-21245, 1999.
603 Goode, J. G., Yokelson, R. J., Ward, D. E., Susott, R. A., Babbitt, R. E., Davies, M. A., and Hao, W. M.:
604 Measurements of excess O_3, CO_2, CO, CH_4, C_2H_4, C_2H_2, HCN, NO, NH_3, HCOOH, CH_3COOH,
605 HCHO, and CH_3OH in 1997 Alaskan biomass burning plumes by airborne Fourier transform infrared
606 spectroscopy (AFTIR), J. Geophys. Res. Atmos., 105, 22147-22166, 2000.
607 Gordon, I. E., Rothman, L. S., Hill, C., Kochanov, R. V., Tan, Y., Bernath, P. F., Birk, M., Boudon, V.,
608 Campargue, A., Chance, K. V., Drouin, B. J., Flaud, J.-M., Gamache, R. R., Hodges, J. T., Jacquemart,
609 D., Perevalov, V. I., Perrin, A., Shine, K. P., Smith , M.-A. H., Tennyson, J., Toon, G. C., Tran, H.,
610 Tyuterev, V. G., Barbe, A., Császár, A. G., Devi, V. M., Furtenbacher, T., Harrison, J. J., Hartmann,
611 J.-M., Jolly, A., Johnson, T. J., Karman, T., Kleiner, I., Kyuberis, A. A., Loos, J., Lyulin, O. M.,
612 Massie, S. T., Mikhailenko, S. N., Moazzen-Ahmadi, N., Müller, H. S. P., Naumenko, O. V., Nikitin,
613 A. V., Polyansky, O. L., Rey, M., Rotger, M., Sharpe, S. W., Sung, K., Starikova, D., S.A.Tashkun, S.
614 A., VanderAuwera, J., Wagner, G., Wilzewski, J., Wcisło, P., Yu, S., and Zak, E. J.: The

HITRAN2016 molecular spectroscopic database, J. Quant. Spectrosc. Radiat. Transfer, 203, 3-69, 2017.

Griffith, D. W. T.: Synthetic calibration and quantitative analysis of gas-phase FT-IR spectra, Appl. Spectrosc., 50, 59-70, 1996.

Griffith, D. W. T.: MALT5 User guide Version 5.5.9 2016.

Griffith, D. W. T., and Jamie, I. M.: Fourier Transform Infrared Spectrometry in Atmospheric and Trace Gas Analysis, Encyclopedia of Analytical Chemistry: Applications, Theory and Instrumentation, 2006.

Griffiths, J. F., Gilligan, M. F., and Gray, P.: Pyrolysis of isopropyl nitrate. I. Decomposition at low temperatures and pressures, Combust. Flame, 24, 11-19, 1975.

Hamada, Y., Nishimura, Y., and Tsuboi, M.: Infrared spectrum of trans-acrolein, Chem. Phys., 100, 365-375, 1985.

Hatch, L. E., Yokelson, R. J., Stockwell, C. E., Veres, P. R., Simpson, I. J., Blake, D. R., Orlando, J. J., and Barsanti, K. C.: Multi-instrument comparison and compilation of non-methane organic gas emissions from biomass burning and implications for smoke-derived secondary organic aerosol precursors, Atmos. Chem. Phys., 17, 1471-1489, 2017.

Herget, W. F., and Brasher, J. D.: Remote measurement of gaseous pollutant concentrations using a mobile Fourier transform interferometer system, Appl. Opt., 18, 3404-3420, 1979.

Hollenstein, H., and Günthard, H. H.: Solid state and gas infrared spectra and normal coordinate analysis of 5 isotopic species of acetaldehyde, Spectrochim. Acta A Mol. Spectrosc., 27, 2027-2060, 1971.

Hosseini, S., Shrivastava, M., Qi, L., Weise, D. R., Cocker, D. R., Miller, J. W., and Jung, H. S.: Effect of low-density polyethylene on smoke emissions from burning of simulated debris piles, J. Air Waste Manag. Assoc., 64, 690-703, 2014.

Jia, C., and Batterman, S.: A critical review of naphthalene sources and exposures relevant to indoor and outdoor air, Int. J. Environ. Res. Public Health, 7, 2903-2939, 2010.

Johnson, T. J., Masiello, T., and Sharpe, S. W.: The quantitative infrared and NIR spectrum of CH_2I_2 vapor: vibrational assignments and potential for atmospheric monitoring, Atmos. Chem. Phys., 6, 2581-2591, 2006.

Johnson, T. J., Sams, R. L., Burton, S. D., and Blake, T. A.: Absolute integrated intensities of vapor-phase hydrogen peroxide (H_2O_2) in the mid-infrared at atmospheric pressure, Anal. Bioanal. Chem., 395, 377-386, 2009.

Johnson, T. J., Sams, R. L., Profeta, L. T., Akagi, S. K., Burling, I. R., Yokelson, R. J., and Williams, S. D.: Quantitative IR spectrum and vibrational assignments for glycolaldehyde vapor: glycolaldehyde measurements in biomass burning plumes, J. Phys. Chem. A, 117, 4096-4107, 2013.

Johnson, T. J., Wienhold, F. G., Burrows, J. P., and Harris, G. W.: Frequency modulation spectroscopy at 1.3 μm using InGaAsP lasers: a prototype field instrument for atmospheric chemistry research, Appl. Opt., 30, 407-413, 1991.

Jonsson, A., and Bertilsson, B. M.: Formation of methyl nitrite in engines fueled with gasoline/methanol and methanol/diesel, Environ. Sci. Technol., 16, 106-110, 1982.

Kabbadj, Y., Herman, M., Di Lonardo, G., Fusina, L., and Johns, J. W. C.: The bending energy levels of C_2H_2, J. Mol. Spectrosc., 150, 535-565, 1991.

Karl, T. G., Christian, T. J., Yokelson, R. J., Artaxo, P., Hao, W. M., and Guenther, A.: The Tropical Forest and Fire Emissions Experiment: method evaluation of volatile organic compound emissions measured by PTR-MS, FTIR, and GC from tropical biomass burning, Atmos. Chem. Phys., 7, 5883-5897, 2007.

Koss, A. R., Sekimoto, K., Gilman, J. B., Selimovic, V., Coggon, M. M., Zarzana, K. J., Yuan, B., Lerner, B. M., Brown, S. S., Jimenez, J. L., Krechmer, J., Roberts, J. M., Warneke, C., Yokelson, R. J., and de Gouw, J.: Non-methane organic gas emissions from biomass burning: identification, quantification, and emission factors from PTR-ToF during the FIREX 2016 laboratory experiment, Atmos. Chem. Phys., 18, 3299, 2018.

Lifshitz, A., Frenklach, M., and Burcat, A.: Structural isomerization $CH_2{=}C{=}CH_2 \rightleftarrows CH_3{-}C{\equiv}CH$. Studies with a single pulse shock tube, J. Phys. Chem., 79, 1148-1152, 1975.

666 Lifshitz, A., Frenklach, M., and Burcat, A.: Pyrolysis of allene and propyne behind reflected shocks, J.
667 Phys. Chem., 80, 2437-2443, 1976.
668 Lindenmaier, R., Williams, S. D., Sams, R. L., and Johnson, T. J.: Quantitative infrared absorption
669 spectra and vibrational assignments of crotonaldehyde and methyl vinyl ketone using gas-phase mid-
670 infrared, far-infrared, and liquid raman spectra: s-cis vs s-trans composition confirmed via temperature
671 studies and ab initio methods, J. Phys. Chem. A, 121, 1195-1212, 2017.
672 Liu, W.-J., Li, W.-W., Jiang, H., and Yu, H.-Q.: Fates of chemical elements in biomass during its
673 pyrolysis, Chem. Rev., 117, 6367-6398, 2017.
674 Lobert, J. M., Scharffe, D. H., Weimin, H., Kuhlbusch, T. A., Seuwen, R., Warneck, P., and Crutzen, P.
675 J.: Experimental evaluation of biomass burning emissions: Nitrogen and carbon containing
676 compounds. Global biomass burning. Atmospheric, climatic, and biospheric implications, 1991.
677 Lord, R. C., and Venkateswarlu, P.: The Rotation-Vibration Spectra of Allene and Allene-d_4, J. Chem.
678 Phys., 20, 1237-1247, 1952.
679 Lu, M., and Mulholland, J. A.: PAH growth from the pyrolysis of CPD, indene and naphthalene mixture,
680 Chemosphere, 55, 605-610, 2004.
681 Mertz, L.: Auxiliary computation for Fourier spectrometry, Infrared Phys., 7, 17-23, 1967.
682 Miller, J. D., Safford, H. D., Crimmins, M., and Thode, A. E.: Quantitative evidence for increasing forest
683 fire severity in the Sierra Nevada and southern Cascade Mountains, California and Nevada, USA,
684 Ecosystems, 12, 16-32, 2009.
685 Orlando, J. J., and Tyndall, G. S.: Mechanisms for the reactions of OH with two unsaturated aldehydes:
686 Crotonaldehyde and acrolein, J. Phys. Chem. A, 106, 12252-12259, 2002.
687 Park, J.-S., Wade, T. L., and Sweet, S.: Atmospheric distribution of polycyclic aromatic hydrocarbons
688 and deposition to Galveston Bay, Texas, USA, Atmos. Environ., 35, 3241-3249, 2001.
689 Phillips, M. C., Taubman, M. S., Bernacki, B. E., Cannon, B. D., Stahl, R. D., Schiffern, J. T., and Myers,
690 T. L.: Real-time trace gas sensing of fluorocarbons using a swept-wavelength external cavity quantum
691 cascade laser, Analyst, 139, 2047-2056, 2014.
692 Profeta, L. T. M., Sams, R. L., Johnson, T. J., and Williams, S. D.: Quantitative infrared intensity studies
693 of vapor-phase glyoxal, methylglyoxal, and 2, 3-butanedione (diacetyl) with vibrational assignments,
694 J. Phys. Chem. A, 115, 9886-9900, 2011.
695 Richter, H., and Howard, J. B.: Formation of polycyclic aromatic hydrocarbons and their growth to
696 soot—a review of chemical reaction pathways, Prog. Energy Combust. Sci., 26, 565-608, 2000.
697 Safdari, M.-S., Rahmati, M., Amini, E., Howarth, J. E., Berryhill, J. P., Dietenberger, M., Weise, D. R.,
698 and Fletcher, T. H.: Characterization of pyrolysis products from fast pyrolysis of live and dead
699 vegetation native to the Southern United States, Fuel, 229, 151-166, 2018.
700 Schmeltz, I., and Hoffmann, D.: Nitrogen-containing compounds in tobacco and tobacco smoke, Chem.
701 Rev., 77, 295-311, 1977.
702 Seinfeld, J. H., and Pandis, S. N.: Atmospheric chemistry and physics: from air pollution to climate
703 change, John Wiley & Sons, 2012.
704 Selimovic, V., Yokelson, R. J., Warneke, C., Roberts, J. M., Gouw, J. d., Reardon, J., and Griffith, D. W.
705 T.: Aerosol optical properties and trace gas emissions by PAX and OP-FTIR for laboratory-simulated
706 western US wildfires during FIREX, Atmos. Chem. Phys., 18, 2929-2948, 2018.
707 Sharpe, S. W., Johnson, T. J., Sams, R. L., Chu, P. M., Rhoderick, G. C., and Johnson, P. A.: Gas-phase
708 databases for quantitative infrared spectroscopy, Appl. Spectrosc., 58, 1452-1461, 2004.
709 Smith, T. E. L., Wooster, M. J., Tattaris, M., and Griffith, D. W. T.: Absolute accuracy and sensitivity
710 analysis of OP-FTIR retrievals of CO_2, CH_4 and CO over concentrations representative of "clean air"
711 and "polluted plumes", Atmos. Meas. Tech., 4, 97-116, 2011.
712 Stein, Y. S., Antal Jr, M. J., and Jones jr, M.: A study of the gas-phase pyrolysis of glycerol, J. Anal.
713 Appl. Pyrolysis, 4, 283-296, 1983.
714 Stockwell, C. E., Yokelson, R., Kreidenweis, S. M., Robinson, A. L., DeMott, P. J., Sullivan, R. C.,
715 Reardon, J., Ryan, K. C., Griffith, D. W. T., and Stevens, L.: Trace gas emissions from combustion of
716 peat, crop residue, domestic biofuels, grasses, and other fuels: configuration and Fourier transform

717 infrared (FTIR) component of the fourth Fire Lab at Missoula Experiment (FLAME-4), Atmos. Chem.
718 Phys., 14, 9727-9754, 2014.
719 Taghizadeh, M. T., Yeganeh, N., and Rezaei, M.: The investigation of thermal decomposition pathway
720 and products of poly (vinyl alcohol) by TG-FTIR, J. Appl. Polym. Sci., 132, 2015.
721 Talbot, R. W., Beecher, K. M., Harriss, R. C., and Cofer, W. R.: Atmospheric geochemistry of formic and
722 acetic acids at a mid-latitude temperate site, J. Geophys. Res. Atmos., 93, 1638-1652, 1988.
723 Taubman, M. S., Myers, T. L., Cannon, B. D., and Williams, R. M.: Stabilization, injection and control of
724 quantum cascade lasers, and their application to chemical sensing in the infrared, Spectrochim. Acta A
725 Mol. Biomol. Spectrosc., 60, 3457-3468, 2004.
726 Turetsky, M. R., Kane, E. S., Harden, J. W., Ottmar, R. D., Manies, K. L., Hoy, E., and Kasischke, E. S.:
727 Recent acceleration of biomass burning and carbon losses in Alaskan forests and peatlands, Nat.
728 Geosci., 4, 27, 2011.
729 U.S. EPA: Health effects notebook for hazardous air pollutants. Retrieved August 29, 2018, 2018, from
730 https://www.epa.gov/haps/health-effects-notebook-hazardous-air-pollutants, January 31, 2018.
731 Vione, D., Barra, S., de Gennaro, G., de Rienzo, M., Gilardoni, S., Perrone, M. G., and Pozzoli, L.:
732 Polycyclic aromatic hydrocarbons in the atmosphere: monitoring, sources, sinks and fate. II: Sinks and
733 fate, Ann. Chim., 94, 257-268, 2004.
734 Wagner, N. L., Dubé, W. P., Washenfelder, R. A., Young, C. J., Pollack, I. B., Ryerson, T. B., and
735 Brown, S. S.: Diode laser-based cavity ring-down instrument for NO_3, N_2O_5, NO, NO_2 and O_3 from
736 aircraft, Atmos. Meas. Tech., 4, 1227-1240, 2011.
737 Wagner, R., Fine, J., Simmons, J. W., and Goldstein, J. H.: Microwave Spectrum, Structure, and Dipole
738 Moment of *s-trans* Acrolein, J. Chem. Phys., 26, 634-637, 1957.
739 Ward, D. E., and Hardy, C. C.: Smoke emissions from wildland fires, Environ. Int., 17, 117-134, 1991.
740 Weise, D. R., Johnson, T. J., and Reardon, J.: Particulate and trace gas emissions from prescribed burns in
741 southeastern US fuel types: Summary of a 5-year project, Fire Saf. J., 74, 71-81, 2015.
742 White, J. U.: Long optical paths of large aperture, JOSA, 32, 285-288, 1942.
743 Williams, P. T., and Williams, E. A.: Fluidised bed pyrolysis of low density polyethylene to produce
744 petrochemical feedstock, J. Anal. Appl. Pyrolysis, 51, 107-126, 1999.
745 Yokelson, R. J., Burling, I. R., Gilman, J. B., Warneke, C., Stockwell, C. E., Gouw, J. d., Akagi, S. K.,
746 Urbanski, S. P., Veres, P., Roberts, J. M., Kuster, W. C., Reardon, J., Griffith, D. W. T., Johnson, T. J.,
747 Hosseini, S., Miller, J. W., Cocker III, D. R., Jung, H., and Weise, D. R.: Coupling field and laboratory
748 measurements to estimate the emission factors of identified and unidentified trace gases for prescribed
749 fires, Atmos. Chem. Phys., 13, 89-116, 2013.
750 Yokelson, R. J., Crounse, J. D., DeCarlo, P. F., Karl, T., Urbanski, S. P., Atlas, E., Campos, T.,
751 Shinozuka, Y., Kasputin, V., Clarke, A. D., Weinheimer, A., Knapp, D. J., Montzka, D. D., Holloway,
752 J., Weibring, P., Flocke, F., Zheng, W., Toohey, D., Wennberg, P. O., Wiedinmyer, C., Mauldin, L.,
753 Fried, A., Richter, D., Walega, J., Jimenez, J. L., Adachi, K., Buseck, P. R., Hall, S. R., and Shetter,
754 R.: Emissions from biomass burning in the Yucatan, Atmos. Chem. Phys., 9, 5785, 2009.
755 Yokelson, R. J., Griffith, D. W. T., and Ward, D. E.: Open-path Fourier transform infrared studies of
756 large-scale laboratory biomass fires, J. Geophys. Res. Atmos., 101, 21067-21080, 1996.
757 Yokelson, R. J., Susott, R., Ward, D. E., Reardon, J., and Griffith, D. W. T.: Emissions from smoldering
758 combustion of biomass measured by open-path Fourier transform infrared spectroscopy, J. Geophys.
759 Res. Atmos., 102, 18865-18877, 1997.

760

761

762

763